Combining Lanekeeping and Vehicle Following with Hazard Maps

J. Christian Gerdes
Design Division
Department of Mechanical Engineering
Stanford University
Stanford, California 94305-4021
Email: gerdes@cdr.stanford.edu

Eric J. Rossetter
Design Division
Department of Mechanical Engineering
Stanford University
Stanford, California 94305-4021
Email: ejross@cdr.stanford.edu

Ursina Saur
ETH
Zurich, Switzerland

Abstract

This paper addresses the issues involved with including moving obstacles in a hazard map or potential field framework for driver assistance systems. Under such a framework, control forces must consist of either conservative forces obtained from the gradient of a potential or artificial damping. By treating vehicle following as a combination of a safety distance and a hazard or potential function, common following strategies, such as constant time headway and guaranteed collision avoidance, can be incorporated into this framework without modification. When combining these fields with lateral potential fields for lanekeeping, however, challenges arise due to the natural asymmetry between the longitudinal and lateral velocity of a vehicle. For instance, a decision to change lanes while approaching a slow moving vehicle results in a large amount of undesirable energy transfer into the lateral dynamics. By treating the lateral and longitudinal hazards - described in road-fixed coordinates - as decoupled, however, such transfers can be eliminated. Because of the manner in which the lateral and longitudinal dynamics couple, control with decoupled hazard maps resembles the coupled case when following or lanekeeping while eliminating the problems associated with energy transfer. The paper concludes by discussing the characteristics of the dynamic equations that lead to this result and outlining future work in obtaining rigorous hazard bounds for the decoupled controller.

1 Introduction

As vehicle safety systems expand to encompass functions such as stability control, lanekeeping and collision avoidance, tighter integration of these control tasks is required. To meet this challenge, several paradigms for systems integration have been proposed. Hennessey *et al.* (1995) looked at combining control objectives using the framework of "virtual

bumpers". In this approach, the vehicle behaved as if there were imaginary springs and dampers attached to the vehicle's center. While a simple idea intuitively, Hennessey *et al.* (1995) detailed complexities that can arise with bifurcations and Schiller *et al.* (1998*b*) noted that tuning stiffnesses can be a challenge when lanekeeping and collision avoidance objectives were combined.

Reichardt and Schick (1994) proposed controlling an autonomous vehicle in a complex environment by assigning a hazard to different points in the environment. This hazard map then became a potential function with vehicle motion controlled to match the gradient of the map. In this way, the vehicle always moved towards less hazardous environmental states, at least locally. Due to the common notion of hazard no tuning was required, making this approach appealing from the standpoint of weighting safety objectives.

Gerdes and Rossetter (1999) applied this view of hazard maps to driver assistance systems. In this framework, the environment produced a force corresponding to the gradient of the potential function that was applied in concert with the base vehicle dynamics using x-by-wire systems. Under this interpretation of the hazard map, the vehicle was not guaranteed to move in the direction of the gradient since the underlying dynamics were not cancelled. Rather, the overall hazard in the system was guaranteed to be bounded by the initial effective energy (the sum of the real kinetic and artificial potential energy) since the uncancelled dynamics were passive. The worst case scenario was thus for the entire energy of the system to be converted into the artificial potential energy or hazard. The application of this technique was illustrated on a combined lanekeeping and stability control system where all hazards in the environment were considered stationary. This paper extends the previous work to cover moving hazards in the environment, particularly those of other vehicles in the lane ahead. Although collision avoidance with moving potential fields has been studied extensively, the common approach of letting the potential function approach infinity at the obstacle (Khatib 1986) is not feasible for automotive applications. Saturation of the brakes (and other actuators) makes any guarantees of this nature suspect, particularly since the obstacles are capable at decelerating at rates comparable to that of the controlled vehicle. These issues can be resolved by combining a concept of a safety distance for the following vehicle with a hazard - or potential function - associated with deviation from that distance. The design and interpretation of such a control structure in light of previous work in vehicle following is discussed in Section 2. For certain cases, the bound of initial energy is shown to be greatly conservative when predicting maximum hazard.

When the following fields are restricted to a single lane and combined with lateral potential fields for lanekeeping, some drawbacks of a strict potential field controller become apparent. Due to the large asymmetry between longitudinal and lateral velocity, a lane change while in the potential field behind a lead vehicle produces an undesirably large increase in lateral velocity. This can be eliminated by exploiting the asymmetry to apply lanekeeping forces only to the lateral dynamics and following forces only to the longitudinal dynamics. The resulting control structure thus encompasses some of the character of virtual spring stiffnesses in the virtual bumper approach (Hennessey *et al.* 1995, Schiller *et al.* 1998*a*, Schiller *et al.* 1998*b*) with the important distinction that the springs are fixed to the environment and described in lane-fixed coordinates. At the same time, the structure retains the central concept of hazard (Reichardt and Schick 1994, Gerdes and Rossetter 1999), with separate lateral and longitudinal hazards reflecting the fact that driving on a highway is a combination of lanekeeping, following and overtaking, not general 2D motion. Suggestions for a more analytical treatment of this scaled potential field controller conclude the paper.

2 Hazard Maps for Following

Vehicle follower laws have been developed by a number of researchers for applications ranging from collision avoidance to intelligent cruise control (Ioannou and Chien 1993) to highway automation (Shladover 1991). Using the approach of Saur (2000), the vehicle location along a straight roadway is given by s and a vehicle in the lane ahead is represented by a position, s_l. Other terms are defined relative to this position (Figure 1). s_d is a safety distance behind the lead car which is set by the following policy and s_{des} is the desired position for the following car.

$$s_{des} = s_l - s_d \tag{1}$$

The spacing error, ϵ_s, is defined relative to the desired position as:

$$\epsilon_s = s - s_{des} \tag{2}$$

The potential field is then defined as some function $V(\epsilon_s)$. In this representation, the safety distance contains the desired spacing dynamics and the potential field represents the hazard associated with following more closely than the follower law dictates.

The general form suggested by Ioannou and Chien (1993) for a safe distance behind the lead vehicle:

$$s_d = \lambda_1 \left(\dot{s}^2 - \dot{s}_l^2\right) + \lambda_2 \dot{s} + \lambda_3 \tag{3}$$

can be easily cast in the framework of hazard maps by defining a hazard $V(\epsilon_s)$ associated with following more closely than this safe distance. When dealing with multiple lanes, this hazard must be interpolated to zero in some manner outside the lane to reflect the fact that the vehicle occupies only a single lane. Achieving this raises a new set of issues which are treated in Section 3.

For now, we assume that the vehicle behaves like a mass point with one degree of freedom in the longitudinal direction and an equation of motion:

$$m\ddot{s} = u \tag{4}$$

The control input (physically the braking and acceleration forces) is assigned the negative gradient of the potential function or hazard, yielding the closed-loop dynamics

$$m\ddot{s} = -\frac{\partial V}{\partial \epsilon_s} = -\frac{\partial V}{\partial s} \tag{5}$$

To make this controller practical, several constraints on the potential function are useful. First, setting the gradient such that $\partial V/\partial \epsilon_s = 0$ when $\epsilon_s = 0$ ensures that the force applied to the vehicle as it hits the potential field is not discontinuous. Secondly, an increasing gradient with increasing spacing error leads to a gradual increase in brake force. Finally, the peak value of the gradient should be no greater than the maximum braking force of which the vehicle is capable. By adapting the shape of the potential function and choosing different gains in Equation 3, different following behaviors can be obtained.

Constant Time Headway

A constant time headway strategy can be obtained by setting $\lambda_1 = 0$ so

$$s_d = \lambda_2 \dot{s} + \lambda_3 \tag{6}$$

The rate of change of spacing error is given by:

$$\begin{aligned} \dot{\epsilon}_s &= \dot{s} - \dot{s}_l + \lambda_2 \ddot{s} \\ &= \dot{s} - \dot{s}_l - \frac{\lambda_2}{m} \frac{\partial V}{\partial \epsilon_s} \end{aligned} \tag{7}$$

The rate of change of kinetic and potential energy are

$$\dot{T} = m\dot{s}\ddot{s} = -\frac{\partial V}{\partial \epsilon_s}\dot{s} \tag{8}$$

$$\dot{V} = \frac{\partial V}{\partial \epsilon_s}\dot{s} - \frac{\partial V}{\partial \epsilon_s}\dot{s}_l - \frac{\lambda_2}{m}\left(\frac{\partial V}{\partial \epsilon_s}\right)^2 \tag{9}$$

The change of artificial potential energy or hazard contains three terms: the conservative transfer from kinetic energy and two nonconservative terms related to the motion of the potential field. The first of these nonconservative terms relates to the fact that the lead vehicle motion "pulls" the potential field along the roadway while the second relates to the motion of the potential field due to the time headway. Combining these equations, the total energy change is the sum of the nonconservative terms:

$$\dot{E} = -\frac{\partial V}{\partial \epsilon_s}\dot{s}_l - \frac{\lambda_2}{m}\left(\frac{\partial V}{\partial \epsilon_s}\right)^2 \tag{10}$$

If the lead vehicle is not moving in reverse, these terms clearly remove energy from the system, so the total hazard is bounded by the initial energy.

In fact, the maximum hazard will be less than the initial total energy since these damping terms are not negligible. A better bound on hazard can be obtained for a particular shape of the potential function. For instance, with a quadratic potential function

$$V(\epsilon_s) = \frac{1}{2} c_0 {\epsilon_s}^2 \tag{11}$$

the dynamics are given by

$$\dot{\epsilon}_s = \dot{s} - \dot{s}_l - \frac{\lambda_2}{m} c_0 \epsilon_s \tag{12}$$

$$\begin{aligned} \ddot{\epsilon}_s &= \ddot{s} - \ddot{s}_l - \frac{\lambda_2}{m} c_0 \dot{\epsilon}_s \\ &= -\frac{c_0}{m}\epsilon_s - \ddot{s}_l - \frac{\lambda_2}{m} c_0 \dot{\epsilon}_s \end{aligned} \tag{13}$$

so

$$\ddot{\epsilon}_s + \frac{\lambda_2 c_0}{m}\dot{\epsilon}_s + \frac{c_0}{m}\epsilon_s = -\ddot{s}_l \tag{14}$$

This can be solved for the maximum spacing error (and hence hazard) given any initial speed mismatch $\dot{\epsilon}_s$ and lead vehicle deceleration $\ddot{s}_l$. As Figure 2 illustrates, the maximum potential energy can be considerably less than the initial energy. This plot demonstrates the transfer from kinetic to artificial potential energy for a vehicle following a lead vehicle at 30 m/s with a 2 second headway after the lead vehicle begins to decelerate at 4 m/s^2.

These simulations were performed using a simple vehicle model (Gerdes and Rossetter 1999) together with a modified Dugoff tire model (Guntur and Sankar 1980). The conservative nature of the energy bound follows from the motion of the lead vehicle and the time headway. In the event that both the time headway and the lead vehicle velocity are zero (corresponding to a constant desired safety distance and a "brick-wall" stop by the lead vehicle), the kinetic energy is transferred entirely into the hazard (Figure 3).

There are several points to note about this controller. First, while the potential field framework is generally associated with conservative forces, the construction of the artificial hazard around a safety distance that depends upon speed can inject damping into the system. Secondly, the shape of the potential function and the time headway are independent design parameters. Together they determine the absolute level of hazard experienced by the vehicle and the spacing error dynamics.

Conservative Safety Distance

A more conservative safety distance that can guarantee collision avoidance can be obtained with $\lambda_1 = 1/2d$ and $\lambda_2 = 0$:

$$s_d = \frac{1}{2d}\left(\dot{s}^2 - \dot{s}_l^2\right) + \lambda_3 \tag{15}$$

where d is the peak deceleration capability of both the leading and following vehicles. This strategy results in a spacing error given by

$$\dot{\epsilon}_s = \dot{s} - \dot{s}_l + \frac{1}{d}\left(\dot{s}\ddot{s} - \dot{s}_l\ddot{s}_l\right) \tag{16}$$

The rate of change of kinetic energy is the same as in the constant time headway case while the rate of change of potential energy is

$$\begin{aligned} \dot{V} &= \frac{\partial V}{\partial \epsilon_s}\left(\dot{s} + \frac{1}{d}\dot{s}\ddot{s}\right) + \frac{\partial V}{\partial \epsilon_s}\left(-\dot{s}_l + \frac{1}{d}\dot{s}_l\ddot{s}_l\right) \\ &= \frac{\partial V}{\partial \epsilon_s}\dot{s} - \frac{1}{md}\left(\frac{\partial V}{\partial \epsilon_s}\right)^2 \dot{s} + \frac{\partial V}{\partial \epsilon_s}\left(\alpha - 1\right)\dot{s}_l \end{aligned} \tag{17}$$

where

$$\alpha = -\frac{\ddot{s}_l}{d} \leq 1 \tag{18}$$

This can also be bounded, though in a slightly different manner than the constant time headway case. From Equation 17, $\dot{V}$ is a maximum - not surprisingly - when the lead vehicle decelerates at its maximum level d. If the potential function has been designed to have a gradient equal to zero at zero spacing error and increasing thereafter as suggested, the rate of change of hazard goes to zero when

$$\frac{\partial V}{\partial \epsilon_s} = md \tag{19}$$

Figure 4 illustrates this follower law for the same set of conditions as Figure 2 with $d = 4m/s^2$. Since more conservatism has been introduced by this choice of the safety distance, the maximum hazard is even less than the constant time headway cases presented before.

3 Moving Hazards in 2D - Coupled Hazard Maps

Incorporating the hazard interpretation of vehicle following in a framework that includes lanekeeping and lane changing requires a bit of extension beyond what was presented in the previous section. First, the model and control law must be extended to include yaw and lateral dynamics as briefly developed below (and in more detail in Gerdes and Rossetter (1999)). Secondly, the field associated with the lead vehicle must be truncated outside the lane to enable overtaking maneuvers. This is accomplished by a multiplicative shaping function on the follower potential function.

Vehicle and Environment Models

The vehicle model (Figure 5) is a simple yaw plane representation with three degrees of freedom (Koepele and Starkey 1990) and differential braking capability. While the double-track model is used for the purposes of differential braking, we assume that the left and right tires possess the same slip angle (in other words, a simple bicycle model for the kinematics). Assuming a vehicle with throttle-, brake- and steer-by-wire capability, the equations of motion are

$$D\ddot{q} = f(\dot{q}) + g(\dot{q}, u_c) \tag{20}$$

where $\dot{q} = [U_x \; U_y \; r]^T$ and $u_c = [\delta \; F_{xrf} \; F_{xlf} \; F_{xrr} \; F_{xlr}]^T$. The positive definite mass matrix, D, is

$$D = \begin{bmatrix} m & 0 & 0 \\ 0 & m & 0 \\ 0 & 0 & I_z \end{bmatrix} \tag{21}$$

and the drift vector f is:

$$f = \begin{bmatrix} mrU_y \\ F_{yr} - mrU_x + \hat{F}_{yf} \\ -bF_{yr} + a\hat{F}_{yf} \end{bmatrix} \tag{22}$$

where

$$\hat{F}_{yf} = -\hat{C}_f \left(\frac{ra + U_y}{U_x} \right) \; sgn(U_x) \tag{23}$$

for some effective cornering stiffness, $\hat{C}_f \geq 0$ and g can be set arbitrarily by control. Using this definition, the drift term f represents system damping since

$$\begin{aligned} \dot{q}^T f &= F_{yr}(U_y - br) + \hat{F}_{yf}(U_y + ra) \\ &= F_{yr}(U_y - br) - \hat{C}_f \frac{(U_y + ra)^2}{|U_x|} \\ &\leq 0 \end{aligned}$$

under the assumption that the tire force and the slip angle are oppositely directed.

For this paper, the environment is modeled simply as a straight section of roadway with the position vector $w = [s \; e \; \psi]^T$ representing the distance down the roadway, the lateral offset, and the heading angle, respectively (Figure 6). The state vector of the system is therefore given in terms of the position variables, w and the velocity vector $\dot{q}$. Transformation

between the environmental and body fixed systems can be achieved through

$$\frac{\partial \dot{w}}{\partial \dot{q}} = \frac{\partial w}{\partial q} = \begin{bmatrix} \cos\psi & -\sin\psi & 0 \\ \sin\psi & \cos\psi & 0 \\ 0 & 0 & 1 \end{bmatrix} \tag{24}$$

Control Law

The controller form proposed by Gerdes and Rossetter (1999) adds a conservative force derivable from the potential function and a general damping term to the existing vehicle dynamics. The general control law is of the form

$$g(\dot{q}, u_c) = B_d(\dot{q}, u_d) + F(w, \dot{q}, u_d) - \left(\frac{\partial V}{\partial w}\frac{\partial w}{\partial q}\right)^T \tag{25}$$

where $B_d(\dot{q}, u_d)$ is the portion corresponding to the driver input and the remaining two terms come from the assistance system. $V(w,t)$ is the potential function describing the overall hazard in the environment and $F(w, \dot{q}, u_d)$ is a generalized damping term. This term can be any vector function that satisfies

$$\dot{q}^T F(w, \dot{q}, u_d) \leq 0 \tag{26}$$

Here it is simply set to zero. The driver commands, u_d, consist of the steering wheel, δ_d, the accelerator pedal, F_{ad}, and the brake pedal, F_{bd}. The complete driver command vector is

$$u_d = [\delta_d \; F_{ad} \; F_{bd}]^T \tag{27}$$

If we set

$$B_d(\dot{q}, u_d) \doteq g(\dot{q}, \begin{bmatrix} \delta_d \\ -\frac{F_{bd}}{4} \\ -\frac{F_{bd}}{4} \\ \frac{F_{ad}}{2} - \frac{F_{bd}}{4} \\ \frac{F_{ad}}{2} - \frac{F_{bd}}{4} \end{bmatrix}) \tag{28}$$

then the vehicle will respond to driver inputs as if it had rear-wheel drive and standard connections (ignoring brake proportioning). With full x-by-wire capability, other mappings from driver inputs to control inputs are possible but this represents the simplest choice.

It can be shown that if the following relation holds for the follower law:

$$\frac{\partial V}{\partial \epsilon_s}(-\dot{s}_l + \dot{s}_d) \leq 0 \tag{29}$$

the combination of kinetic energy and artificial potential energy is always decreasing in the absence of driver input. Hence the results of Gerdes and Rossetter (1999) can be simply extended. As discussed below, however, this condition is difficult to strictly enforce (though generally true). A larger problem, however, exists with the coupling between lateral and longitudinal fields.

Simulation of Coupled Controller

The particular potential function chosen to illustrate the combination of fixed and moving hazards in two dimensions has the form:

$$V = V_e(e) + V_\epsilon(\epsilon_s)V_l(e) \tag{30}$$

where V_e is the lanekeeping potential field, V_ϵ is the vehicle following field and V_l shapes the vehicle field to match the lane. Without the shaping function V_l, the longitudinal hazard would exist at all lateral positions and not only in the lane of the leading vehicle.

The function V used in the simulations is shown in Figure 7 and represents a combination of the 2 second time headway controller for a vehicle in the right lane with lanekeeping fields as used in Gerdes and Rossetter (1999). The lanekeeping fields are designed for two lanes of traffic travelling in the same direction and the lead vehicle is in the right lane at a spacing error of $20m$. Note that the illustration in Figure 7 is not to scale; the height of the longitudinal fields, which are orders of magnitude larger than those required for lanekeeping, have been decreased in the figure to make the lateral fields visible. With this form of potential function, the equations of motion of the vehicle in global coordinates become:

$$m\ddot{s} = -V_l\frac{\partial V_\epsilon}{\partial \epsilon_s} - \left(F_{yr} + \hat{F}_{yf}\right)\sin\psi \tag{31}$$

$$I_z\ddot{\psi} = -bF_{yr} + a\hat{F}_{yf} \tag{32}$$

$$m\ddot{e} = -\left(\frac{\partial V_e}{\partial e} + V_\epsilon\frac{\partial V_l}{\partial e}\right) + \left(F_{yr} + \hat{F}_{yf}\right)\cos\psi \tag{33}$$

A closer examination of Figure 7 reveals a major obstacle to merging lanekeeping and vehicle following. As the vehicle moves closer to the lead vehicle, the hazard increases sharply. If the driver changes lanes after entering the vehicle following field, the potential field controller translates this artificial potential energy into kinetic energy by greatly increasing the lateral velocity. The effects of this can be seen in the solid lines of Figure 8 which shows a driver-induced lane change initiated at 3 sec, slightly after the following vehicle is influenced by the potential field. The controller moves the car out of the right hand lane, but overshoots the left hand lane, plowing through the potential field on the opposite side.

This difficulty arises due to the inherent asymmetry of vehicle dynamics. Most of the kinetic energy is associated with the longitudinal momentum, so the potential energy grows fairly large during braking. In contrast, only a small distance is necessary to change lanes, resulting in a very high gradient in the lateral direction and a large increase in lateral momentum. This behavior, while necessary to ensure that the total energy decreases, is not particularly acceptable or helpful as a driver assistance system. There is no particular reason why the rapid reduction in hazard needs to be applied as a lateral force as opposed to simply being dissipated. Similarly, the steep gradient in the lateral direction produces far more force than is necessary to prevent the following vehicle from a sideswipe collision with the leading vehicle as it continues the overtaking maneuver. Since most of the energy is associated with longitudinal motion, a lower gradient is sufficient to keep the car in its own lane. These issues are analagous to the points raised by Schiller *et al.* (1998*b*) with regards to the difficulty in tuning virtual bumper springs so that collision avoidance did not

force the vehicle out of the lane. A similar effect would be seen for this controller if the lanekeeping potential fields were applied to curved roads as opposed to the straight segments under consideration here.

4 Moving Hazards in 2D - Decoupled Hazard Maps

This problem can be resolved by removing the gradient of the follower potential field from the control law in the lateral direction. This is equivalent to treating the hazard maps as decoupled, with one map for longitudinal hazards and the other for lateral hazards. The equations of motion become:

$$m\ddot{s} = -V_l \frac{\partial V_\epsilon}{\partial \epsilon_s} - \left(F_{yr} + \hat{F}_{yf}\right) \sin\psi \tag{34}$$

$$I_z \ddot{\psi} = -bF_{yr} + a\hat{F}_{yf} \tag{35}$$

$$m\ddot{e} = -\frac{\partial V_e}{\partial e} + F_{yr} + \hat{F}_{yf} \tag{36}$$

As can be seen from the dashed line in Figure 8, this prevents the dramatic increase in lateral velocity when changing lanes so the driver can successfully execute a lane change. Furthermore, this decoupling causes very little change in the behavior of the system for combined lanekeeping and following within a lane, as demonstrated in Figure 9 where the decoupled and coupled cases are indistinguishable. This figure depicts a following vehicle approaching a slower vehicle with a side disturbance of $200N$ (a wind or side slope) pushing the vehicle into the lateral hazard.

To see why this is the case, consider the form of the coupled equations of motion in the yaw direction. When the rear tire is assumed to be in the linear region,

$$F_{yr} = -C_r \left(\frac{U_y - br}{U_x}\right) \tag{37}$$

and the equations of motion in road-fixed coordinates are:

$$m\ddot{e} = -\frac{\partial V_e}{\partial e} - \frac{(\hat{C}_f + C_r)}{U_x}\dot{e} + (\hat{C}_f + C_r)\sin\psi + \frac{(bC_r - a\hat{C}_f)}{U_x}\cos\psi\dot{\psi} \tag{38}$$

$$I_z \ddot{\psi} = \frac{(bC_r - a\hat{C}_f)}{U_x \cos\psi}\dot{e} - (bC_r - a\hat{C}_f)\tan\psi - \frac{(b^2 C_r + a^2 \hat{C}_f)}{U_x}\dot{\psi} \tag{39}$$

Several observations can be made about this system of equations. First, the linearized form of these equations is a stable system, or can be stabilized by shifting the application point of the virtual force in front of the neutral steer point and adding damping as desired((Rossetter and Gerdes 2000)). Thus, the values of e and ψ, and consequently any hazards containing these values, must be bounded. Second, because the hazards or potentials are described in road-fixed coordinates, the longitudinal velocity, U_x, enters only in the denominator of several damping terms as opposed to contributing a term involving the cross product with the yaw rate (as in the case of vehicle-fixed coordinates). Thus, the yaw and lateral dynamics in road-fixed coordinates are themselves approximately decoupled from the longitudinal dynamics. Similarly, the longitudinal dynamics are given by:

$$m\ddot{s} = -V_l \frac{\partial V_\epsilon}{\partial \epsilon_s} - \left(F_{yr} + \hat{F}_{yf}\right) \sin\psi \tag{40}$$

With the yaw rate and lateral velocity bounded by virtue of the stability of the lateral and yaw dynamics, the side force terms contribute a bounded disturbance. Bounded longitudinal hazard can thus be established using the techniques of the one-dimensional case developed earlier in the paper.

It might appear that this solution throws out the very concept of unified hazard that motivated this work. With the hazard maps decoupled in the controller, the overall decrease of energy (kinetic plus artificial potential) is no longer guaranteed. We can, however, establish bounds on the hazard experienced in the lateral and longitudinal directions, therefore decoupling the problem. Thus we can design combined controllers by setting lanekeeping fields and the lateral and longitudinal components of moving obstacle fields such that the level of hazard produced by specified operating conditions lies beneath an acceptable bound. This is in some sense similar to tuning the springs and dampers of a virtual bumper design, though these springs are attached to global coordinates, move relative to a desired safety distance and can be related to a uniform notion of hazard. The separation of lateral and longitudinal hazards also fits well with the concept that vehicles move in lanes and not on arbitrary paths in two dimensions. Furthermore, the uniform notion of hazard also gives a specific numerical objective to the design procedure. Obtaining the least conservative hazard bounds possible for system design is a topic of current research.

5 Conclusions / Future Work

By incorporating a safety distance with a potential function, the idea of environmental hazards suggested by Reichardt and Schick (1994) and developed into assistance systems by Gerdes and Rossetter (1999) can be extended to include moving vehicles. In this formulation, a variety of existing follower laws can be incorporated into the framework of a hazard map and combined with lanekeeping functions in the form of a lateral hazard map. We believe that such a formulation offers several advantages:

1. The hazard map provides a common measure for examining and weighting vehicle control actions.

2. The approach nicely decouples longitudinal and lateral hazards for the purpose of design.

3. When extending system integration into regions of tire saturation, the hazard value could provide useful information on how to saturate by weighting the relative importance of lateral position, longitudinal position and yaw.

References

Gerdes, J.C. and E.J. Rossetter (1999). A unified approach to driver assistance systems based on artificial potential fields. In: *Proceedings of the 1999 ASME IMECE, Nashville, TN.*

Guntur, R. and S. Sankar (1980). A friction circle concept for dugoff's tyre friction model. *International Journal of Vehicle Design* **4**(1), 373–377.

Hennessey, M., C. Shankwitz and M. Donath (1995). Sensor based 'virtual bumpers' for collision avoidance: Configuration issues. In: *Proceedings of the SPIE.* Vol. 2592.

Ioannou, P.A. and C.C. Chien (1993). Autonomous intelligent cruise control. *IEEE Transactions on Vehicular Technology*.

Khatib, O. (1986). Real-time obstacle avoidance for manipulators and mobile robots. *International Journal of Robotics Research* **5**(1), 90–98.

Koepele, B. and J. Starkey (1990). Closed-loop vehicle and driver models for high-speed trajectory following. In: *Transportation Systems - 1990 ASME WAM, Dallas, TX*. pp. 59–68.

Reichardt, D. and J. Schick (1994). Collision avoidance in dynamic environments applied to autonomous vehicle guidance on the motorway. In: *Proceedings of the IEEE Intelligent Vehicles Symposium, Paris, France*.

Rossetter, E.J. and J.C. Gerdes (2000). The role of handling characteristics in driver assistance systems with environmental interaction. In: *Proceedings of the 2000 ACC, Chicago, IL*.

Saur, U. (2000). Assessment of performance and safety of chassis control systems using a "potential fields" approach. Master's thesis. ETH Zurich.

Schiller, B., V. Morellas and M. Donath (1998*a*). Collision avoidance for highway vehicles using the virtual bumper controller. In: *Proceedings of the 1998 IEEE International Symposium on Intelligent Vehicles, Stuttgart, Germany*.

Schiller, B., Y. Du, D. Krantz, C. Shankwitz and M. Donath (1998*b*). *Vehicle Guidance Architecture for Combined Lane Tracking and Obstacle Avoidance*. Chap. 7 in Artifical Intelligence and Mobile Robots: Case Studies of Successful Robot Systems, pp. 159–192. AIII Press/The MIT Press. Cambridge, MA.

Shladover, S. E. (1991). Longitudinal control of automotive vehicles in close-formation platoons. ASME *Journal of Dynamic Systems, Measurement, and Control* **113**, 231–241.

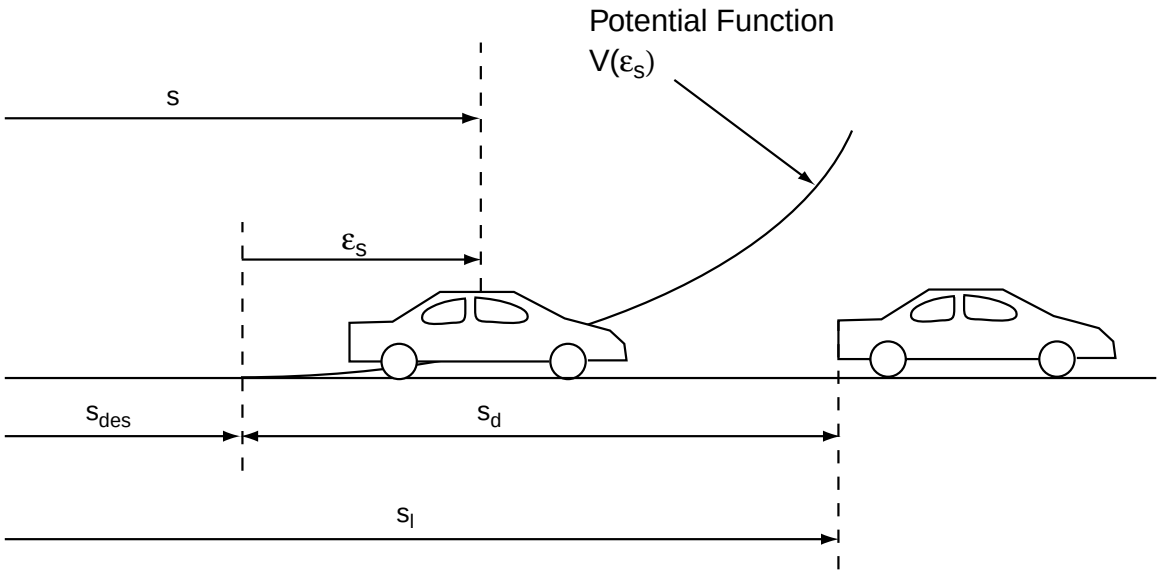

Figure 1: Vehicle spacing parameters

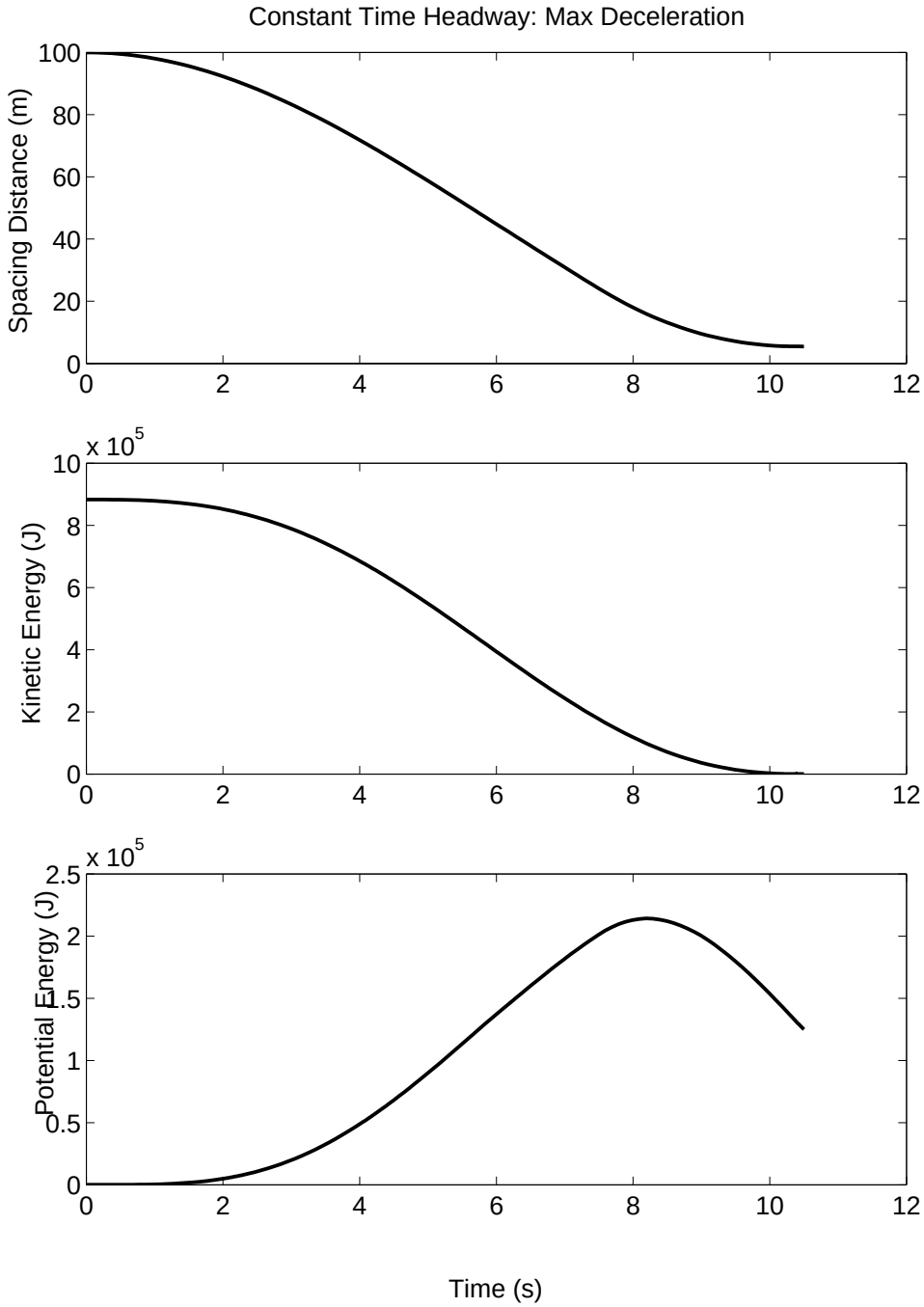

Figure 2: 4 m/s^2 deceleration at $30m/s$, $\lambda_2 = 2$

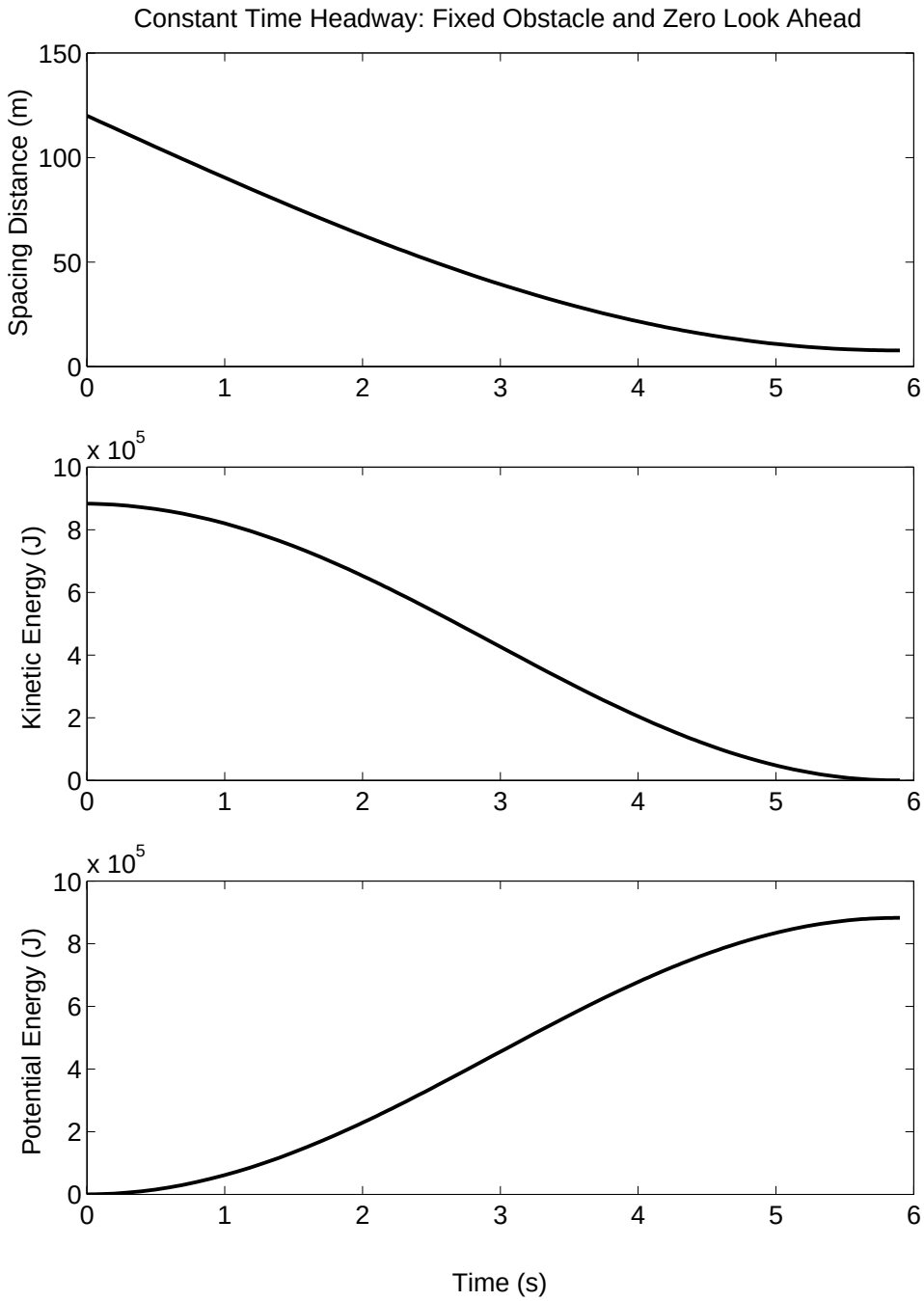

Figure 3: 'Brick wall' stop at $30m/s$, $\lambda_2 = 0$

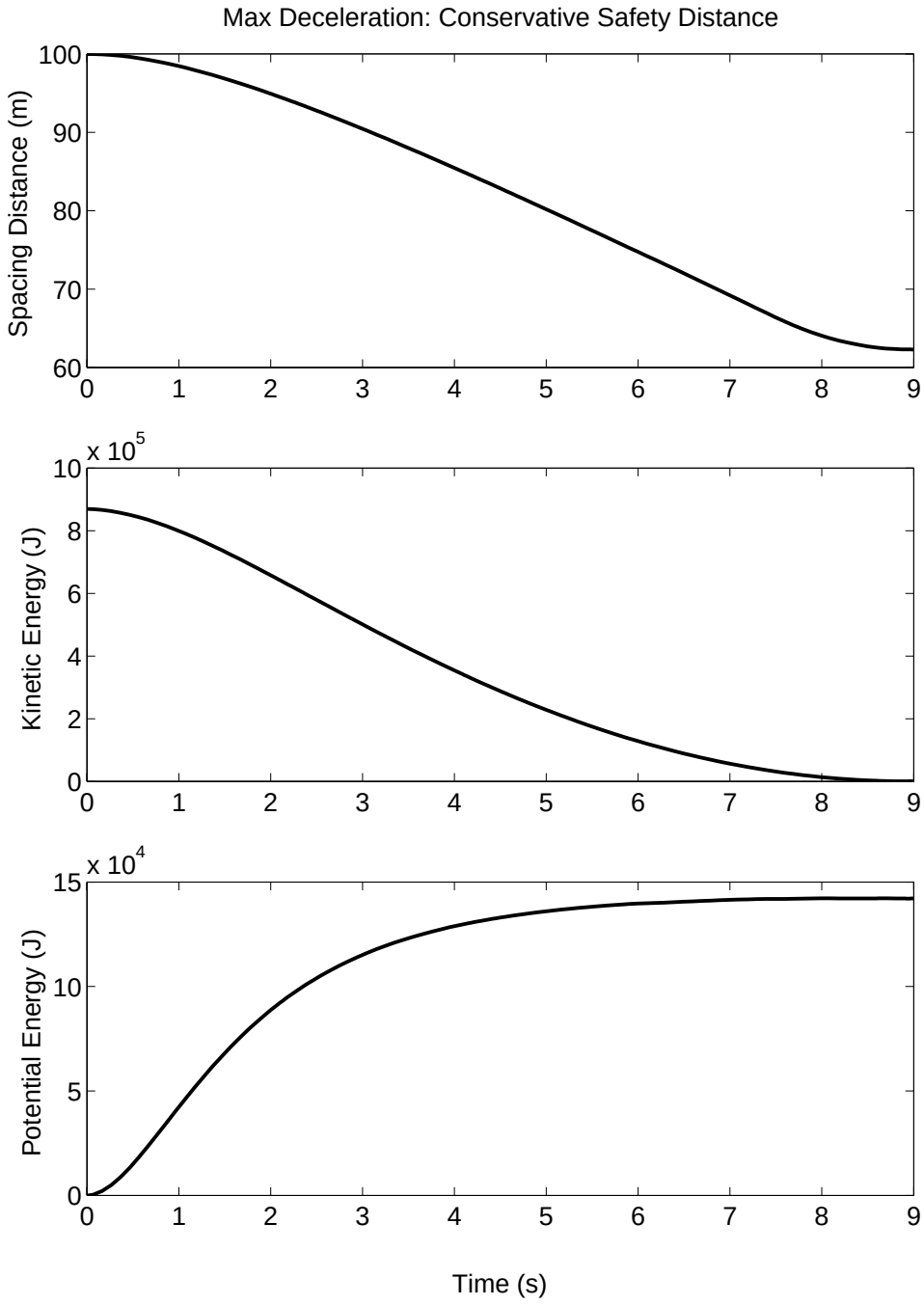

Figure 4: 4 m/s^2 deceleration at $30m/s$, $d = 4m/s^2$

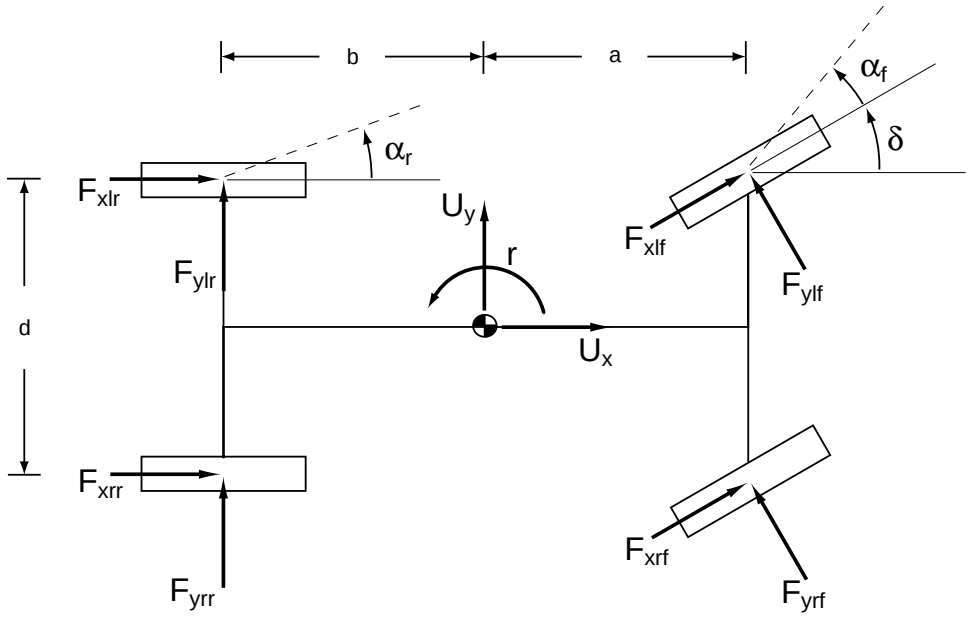

Figure 5: Planar Model of Vehicle Dynamics

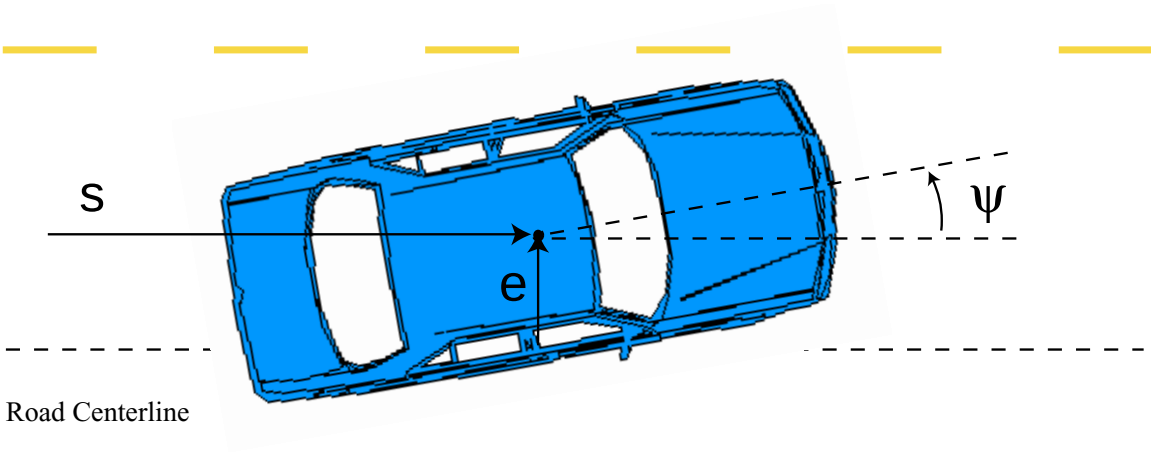

Figure 6: Global Coordinates

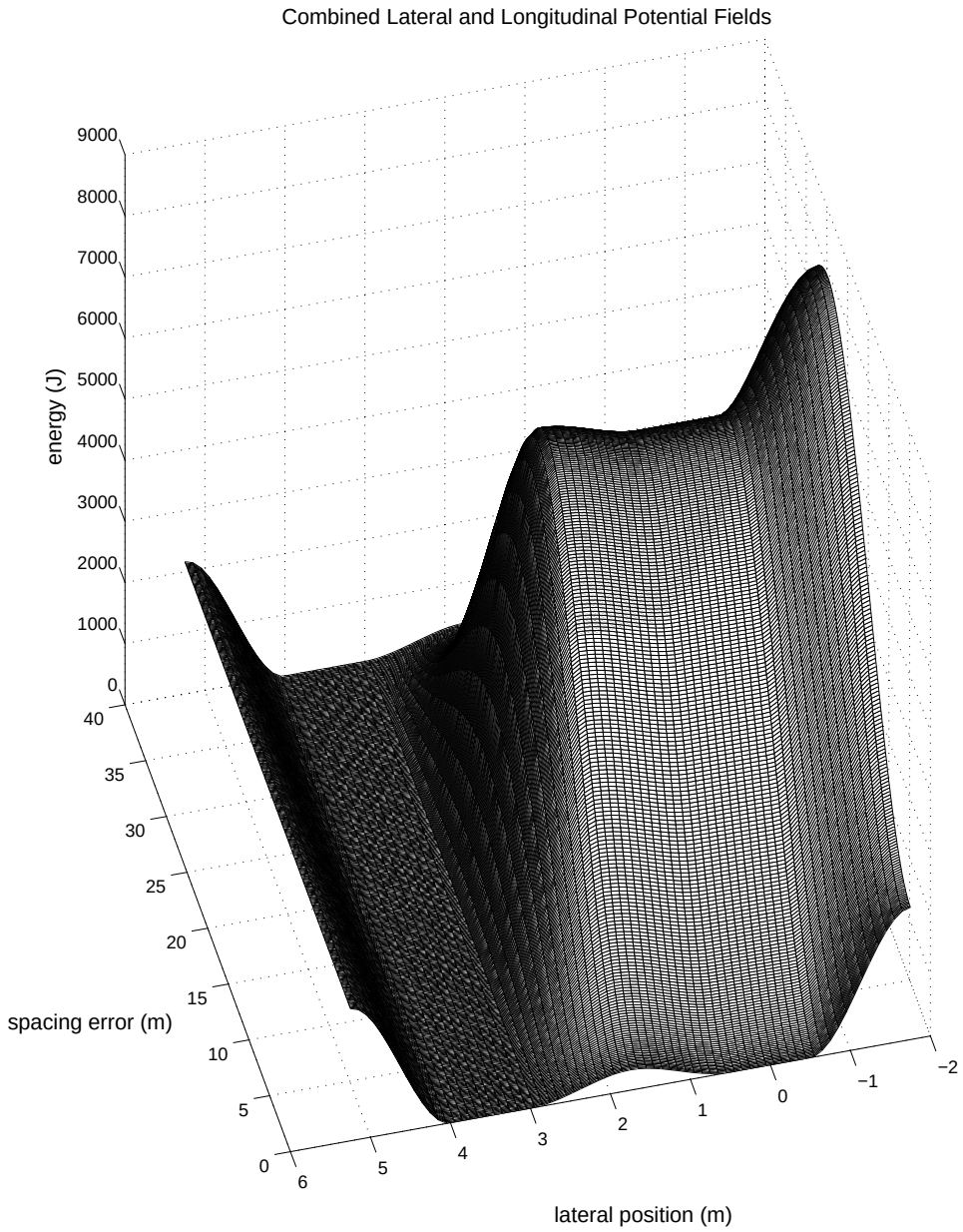

Figure 7: Combined Potential Function

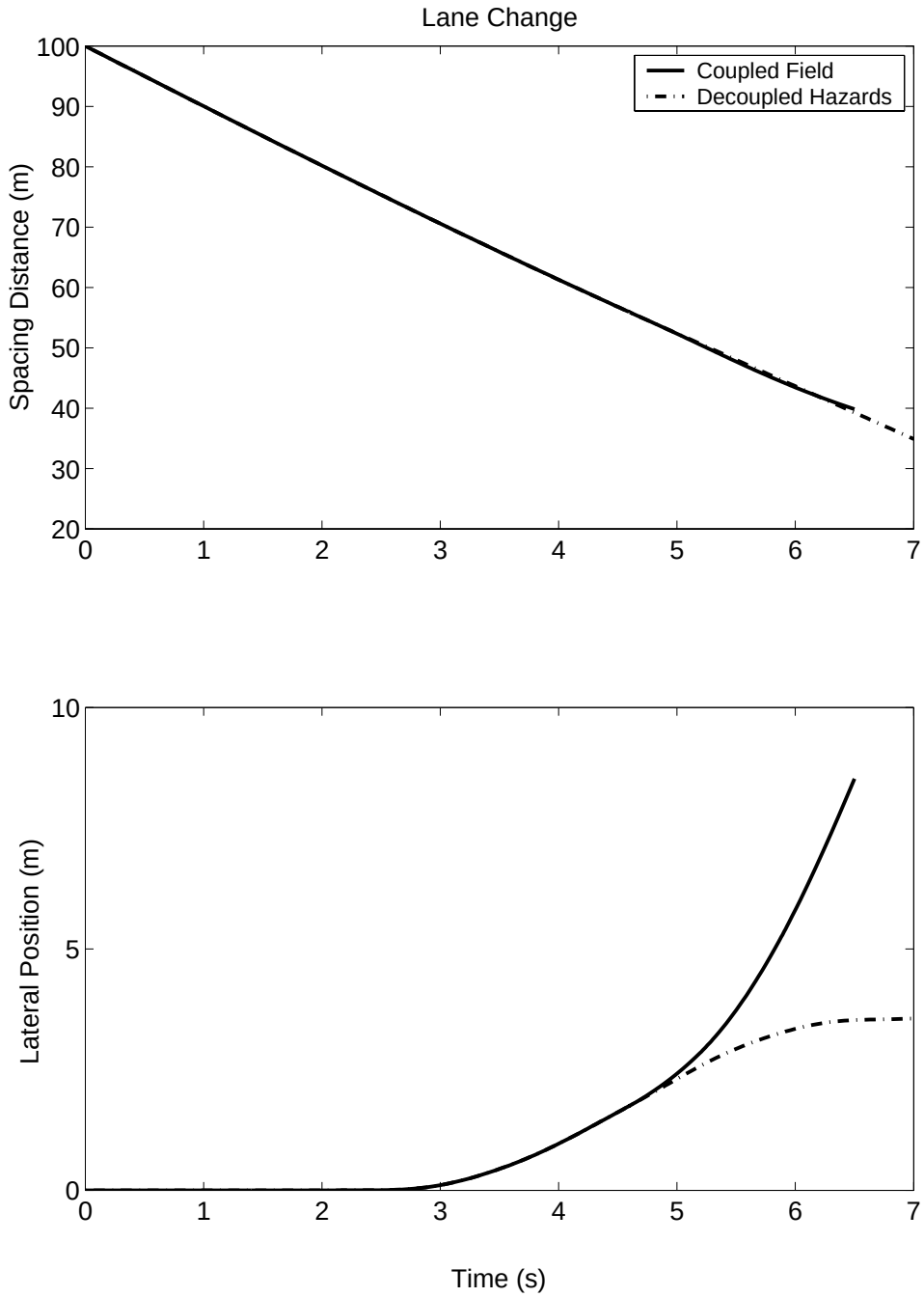

Figure 8: Driver Lane Change with Combined Fields

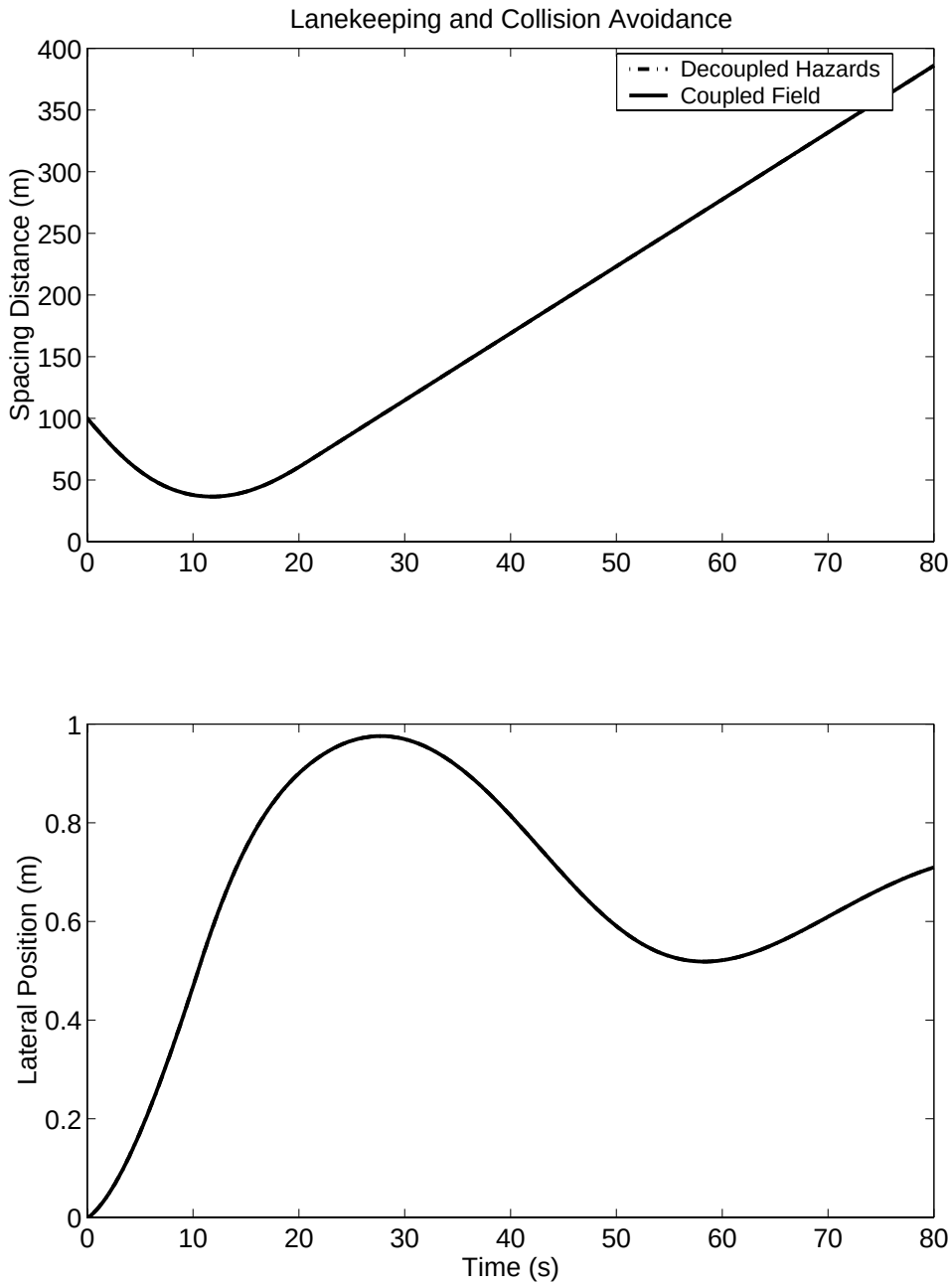

Figure 9: Lanekeeping During Approach